ELSEVIER

Journal of Hazardous Materials B129 (2006) 228–233

Journal of Hazardous Materials

www.elsevier.com/locate/jhazmat

Novel activated alumina-supported iron oxide-composite as a heterogeneous catalyst for photooxidative degradation of reactive black 5

C.L. Hsueh, Y.H. Huang, C.Y. Chen *

Department of Chemical Engineering, National Cheng Kung University, Tainan City 701, Taiwan

Received 19 May 2005; received in revised form 16 August 2005; accepted 25 August 2005
Available online 29 September 2005

Abstract

A novel activated alumina-supported iron oxide-composite (denoted as FeAA-500) was prepared by so-called fluidized-bed reactor (FBR) crystallization. X-ray powder diffraction (XRD), N_2 adsorption/desorption, scanning electron microscopy (SEM) and energy dispersive X-ray spectroscopy (EDX) were used to characterize the FeAA-500. The photo-catalytic activity of the FeAA-500 was evaluated in the photooxidative degradation of 0.1 mM azo-dye reactive black 5 (RB5) in the presence of H_2O_2 and UVA light ($\lambda = 365$ nm) in a solution with a pH of 2.5. Complete decolorization of the model pollutant RB5 was achieved; the total organic carbon (TOC) removal ratio was 95%, and a trace amount of leached ferric ion was detected following 75 min of reaction when 2.0 g/L FeAA-500 was used as a catalyst. FeAA-500 has high photo-catalytic activity; it is therefore a promising heterogeneous photocatalysis of the degradation of organic compounds.

Keywords: Iron oxide; Reactive black 5; Heterogeneous photocatalysis; Decolorization

1. Introduction

Advanced oxidation processes (AOPs) are remediation processes that produce the highly reactive hydroxyl radical ($^{\bullet}$OH) to degrade organic pollutants [1,2]. Since the 1990s, AOPs have attracted considerable attention in relation to wastewater treatment [3–12]. One of the most important AOPs for generating $^{\bullet}$OH is the use of the Fe^{2+}/H_2O_2/UV system, wherein the catalytic ferrous ions are dissolved in water. This process is called the homogeneous photo-Fenton process. In this system, Fe^{2+} in solution acts as a homogeneous catalyst. The formation of $^{\bullet}$OH and the photo-reductive regeneration from Fe can be expressed by the following equations [13].

$$H_2O_2 + Fe^{2+} \rightarrow Fe^{3+} + OH^- + {}^{\bullet}OH, \quad k_1 = 40\text{–}60\ M^{-1}\,s^{-1} \tag{1}$$

$$Fe(OH)^{2+} \xrightarrow{h\nu} Fe^{2+} + {}^{\bullet}OH, \quad k_2 = 2 \times 10^{-3} M^{-1}\,s^{-1} \tag{2}$$

However, the homogeneous photo-Fenton process has a marked shortcoming. It produces iron-containing waste sludge whose disposal is difficult and expensive. This disadvantage limits the further application of the homogeneous photo-Fenton process in treating wastewater. Therefore, the heterogeneous photo-Fenton or photo-Fenton-like processes, has been developed by coating Fe ions in iron oxide onto porous solid as a catalyst. It is called a heterogeneous catalyst because it does not dissolve in water [14–21]. For example, Fernandez et al. [14,15] successfully prepared a Fe^{3+}/Nafion membrane catalyst using a simple ion exchange reaction. They exploited the catalyst in the photo-assisted Fenton degradation of Orange II. However, the Nafion-based catalyst is too expensive to be used in practical applications even though the catalyst can be separated easily from solution. Accordingly, Feng et al. [19–22] utilized Laponite RD, rather than the Nafion film. A search on the Internet revealed that the price of Nafion exceeds 2000 US$/kg, whereas that of Laponite RD is less than 40 US$/kg [20,21]. Therefore, heterogeneous catalysts of the photo-Fenton reaction that are much cheaper than Nafion must be sought. Such a catalyst has not only academic importance but also industrial applications.

In this work, an activated alumina-supported iron oxide-composite was prepared by FBR-crystallization technique [23–26], which is cost-effective and has been used full-scale in industrial applications in Taiwan. Activated alumina-supported iron oxide-composite was originally developed as a heteroge-

* Corresponding author. Tel.: +886 6 2757575/62643; fax: +886 6 2344496.
E-mail address: ccy7@ccmail.ncku.edu.tw (C.Y. Chen).

0304-3894/$ – see front matter © 2005 Elsevier B.V. All rights reserved.
doi:10.1016/j.jhazmat.2005.08.044

neous catalyst of the degradation of RB5 in the presence of H_2O_2 and UVA light. Decolorization efficiency, TOC removal ratio and Fe leaching from the catalysts are discussed in detail herein.

2. Experimental

2.1. Materials

RB5 (Color Index no. 20505), $C_{26}H_{21}N_5Na_4O_{19}S_6$, was purchased from Aldrich Chemical Company (Amherst, NY, USA); it was 55% pure, and had a molecular weight of 991.82. The structure of RB5 is presented below. $NaClO_4$ (Merck) and H_2O_2 (Union Chemical) were of analytical reagent grade and were used without further purification. Activated alumina grain was obtained from Alcoa Chemicals. Deionized and doubly distilled water were used throughout this investigation.

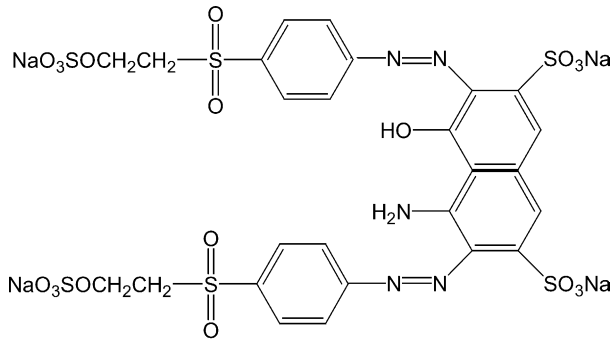

Reactive Black 5 (RB5)

2.2. Preparation of FeAA-500

A novel catalyst, iron oxide on a activated alumina support, was prepared in the following manner [23]. Activated alumina grains were packed in a 30 m^3 FBR (2.1 m Ø × 9 m height). The internal circulation of the FBR was controlled to maintain a upflow superficial velocity of 40 m h^{-1} with a 50% bed expansion. Fig. 1 schematically depicts the apparatus. The bioeffluents of *tannery* wastewater, H_2O_2 and $FeSO_4$ were fed continuously into the reactor bottom. The molar ratio of H_2O_2 to $FeSO_4$ was 2:1. The pH of the solution, which was adjusted by adding dilute aqueous solutions of NaOH or H_2SO_4, was maintained at 3, to prevent the precipitation of $Fe(OH)_3$ [27]. After the reaction had proceeded for around 3 months, iron oxide was coated onto the surface of the activated alumina grains to enable catalytic oxidation. It was then dried overnight in air at 120 °C. Finally, the dried solid was calcined at 500 °C for 24 h.

2.3. Characterization of FeAA-500

FeAA-500 was characterized using a powder diffractometer (Rigaku RX III) with Cu Kα radiation. The accelerating voltage and current were 40 kV and 20 mA. The specific *surface* area of FeAA-500 was measured by the BET method. The sizes of the activated alumina grain support particles and the FeAA-500 particles were obtained using a Hitachi S-400 SEM. The atomic composition of the FeAA-500 surface was elucidated by EDX using an Oxford INCA-400 spectrometer. The total iron concentration was measured using an atomic absorbance spectrophotometer (Hitachi Z-6100).

2.4. Evaluating the photo-catalytic activity of the FeAA-500 catalyst

The model pollutant used to evaluate the FeAA-500 catalyst was an azo-dye RB5. This dye was chosen because it is widely employed in the textile industry and is not biodegradable [28]. The photo-catalytic activity of FeAA-500 in degrading the RB5 solution in a batch photoreactor (Fig. 2) at room temperature was evaluated under illumination at intensity of 1.8 mW cm^{-2}. The irradiation source was a 15 W UVA lamp

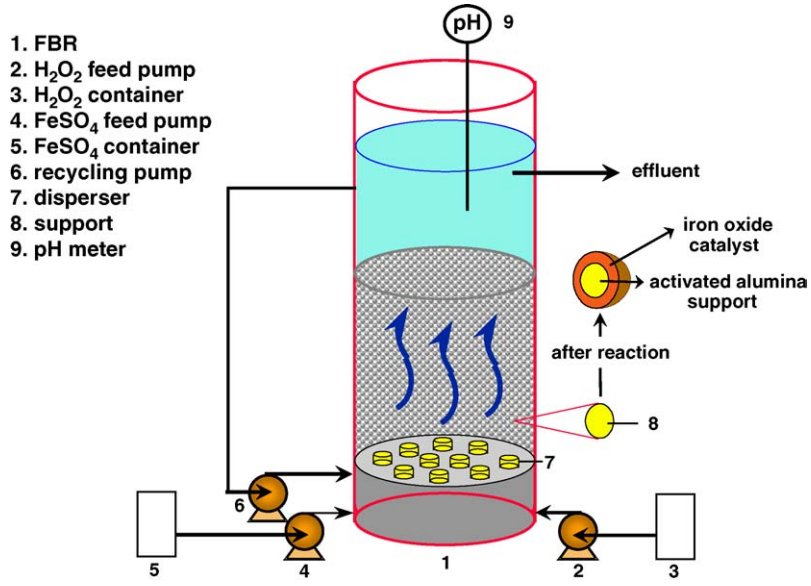

Fig. 1. Schematic diagram of the fluidized-bed reactor.

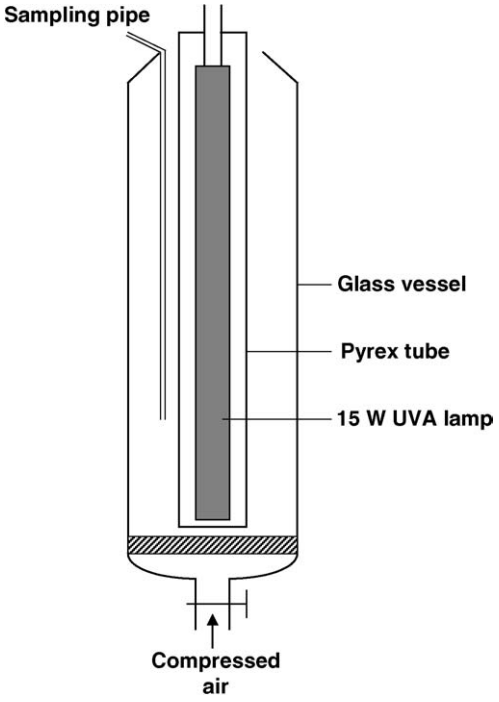

Fig. 2. Schematic diagram of the photoreactor apparatus.

(UVP BL-15 365 nm) fixed inside a cylindrical Pyrex tube (allowing wavelengths $\lambda > 320$ nm to pass). This setup prevented the formation of $^{\bullet}$OH radicals by the direct photolysis of H_2O_2. The total volume of the solution was 1200 mL; the initial concentration of RB5 was 0.1 mM. Specified amounts of $NaClO_4$ and H_2O_2 were dripped into the reactor. The pH of the solution was altered by adding aqueous solutions of NaOH or $HClO_4$. The starting point of the reaction was defined as the time when the UVA light was turned on and a certain quantity of FeAA-500 was added to the photoreactor. Compressed air was bubbled from the bottom at a flow rate of around 1800 mL/min and it was exposed to the ambient air effectively to suspend the catalyst in the reactor and ensure good mixing. Samples were periodically extracted from the reactor using a pipe, and were immediately analyzed using a UV–vis spectrometer after they had been filtered through a 0.25 μm syringe filter made of poly-(vinylidene fluoride) to remove FeAA-500 particles.

The RB5 spectrum showed an absorption peak at 597 nm. Therefore, the concentration of the RB5 solution was determined from the absorption intensity at 597 nm, as determined using a UV–vis spectrometer (Jasco Model 7850). Before the measurement was made, a calibration curve was plotted using standard RB5 of known concentrations. TOC was analyzed using a Shimadzu 500 TOC analyzer.

3. Results and discussion

3.1. Characterization of the FeAA-500 catalyst

Fig. 3 depicts the XRD pattern of the AA-Fe-500. The main diffraction peaks at $2\theta = 33.1^{\circ}$ and 35.6° are assigned to Fe_2O_3 (hematite) crystallite. Accordingly, the XRD analysis demonstrated that the FeAA-500 consists mainly Fe_2O_3 (hematite) crystallite.

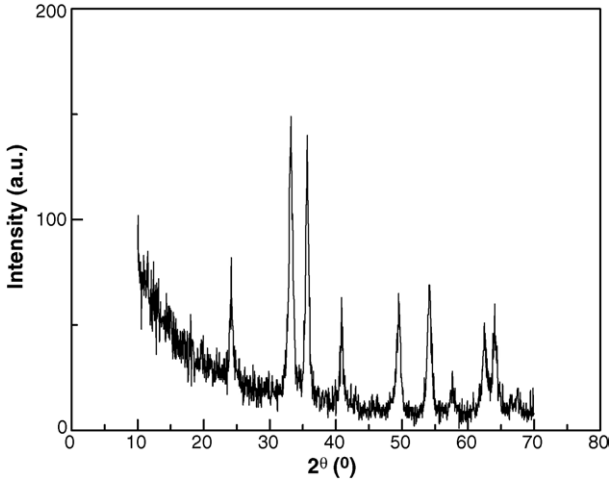

Fig. 3. XRD patterns of the FeAA-500 catalyst.

Table 1
Surface atomic compositions and binding energy (BE) of FeAA-500 determined by EDX

Element	Atomic concentration (at.%)	Binding energy (keV)
C	6.78	0.277
O	45.12	0.525
Al	1.34	1.487
Fe	46.76	0.628, 0.705, 6.404, 7.058

Table 1 presents the surface atomic chemical compositions of FeAA-500 and the binding energy of the detected elements, obtained by EDX. The binding energies of Fe were determined to be 0.628, 0.705, 6.404 and 7.058 keV. Fig. 4 shows the SEM micrographs of the activated alumina grain support and the FeAA-500 prepared using an FBR. Fig. 4a (100×) and b (300×) demonstrate that the shape of the original activated alumina grain support is irregular. It was smoother after the reaction in the FBR had proceeded for 3 months, as displayed in Fig. 4c (100×) and d (500×). The size of the FeAA-500 catalytic particles, determined by SEM, ranged from 80 to 200 μm. Table 2 presents the other characteristics of the FeAA-500 catalyst.

Table 2
Properties of the FeAA-500 catalyst

Parameter	Value
Total iron content of catalyst (g kg^{-1})	346.4
Bulk density (g cm^{-3})	1.19
Absolute (true) density (g cm^{-3})	3.85
Specific surface area (m^2 g^{-1})	154.6
Total pore volume (cm^3 g^{-1})	0.109
Cation-exchange capacities (meq g^{-1})	0.43

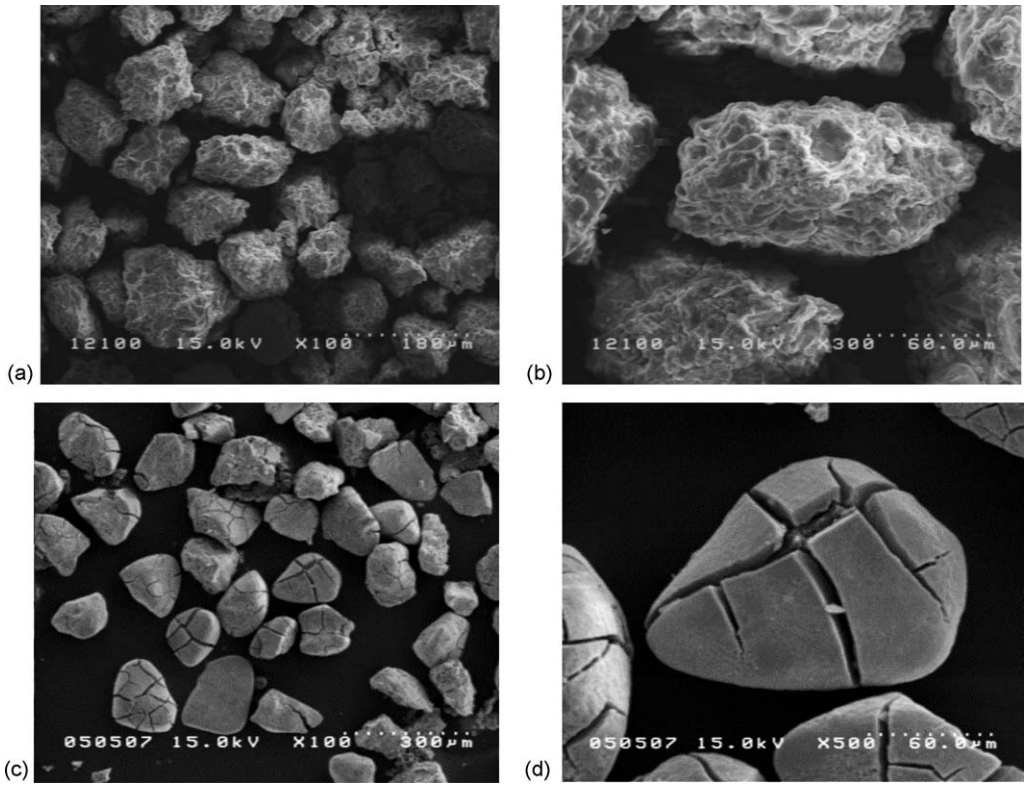

Fig. 4. Scanning electron micrographs of original activated alumina grain support: (a) 100×; (b) 300× and iron oxide; (c) 100×; (d) 500×.

3.2. Evaluation of the photo-catalytic activity of the FeAA-500 catalyst

Numerous investigations have revealed that the solution pH can dramatically influence the heterogeneous photoassisted Fenton degradation of organic compounds. The optimal solution pH has been found to be approximately 3.0 [15,17]. Fig. 5 plots the effect of pH on the degradation of RB5 under UVA light irradiation in the FeAA-500/H_2O_2 system. The figure reveals that a pH of up to 4.5 can be used with FeAA-500 as a catalyst. Moreover, reducing the solution pH from 4.5 to 2.5 considerably promotes the degradation of RB5. The FeAA-500 catalyst was most efficient at a pH of 2.5. Hence, the following experiments were undertaken at pH 2.5 to evaluate the photo-catalytic activity of the FeAA-500 catalyst.

Fig. 6 plots the RB5 concentration against irradiation time, under various conditions. Without H_2O_2 and FeAA-500 catalyst, but with only 15 W UVA (curve a), the RB5 concentration barely

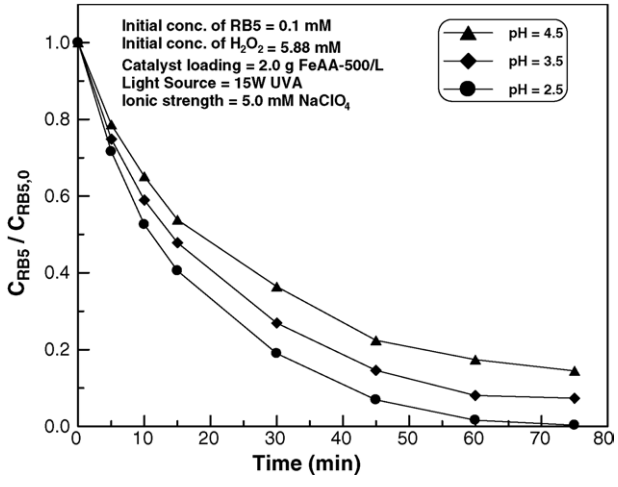

Fig. 5. Effect of the solution pH on the photooxidative degradation of RB5.

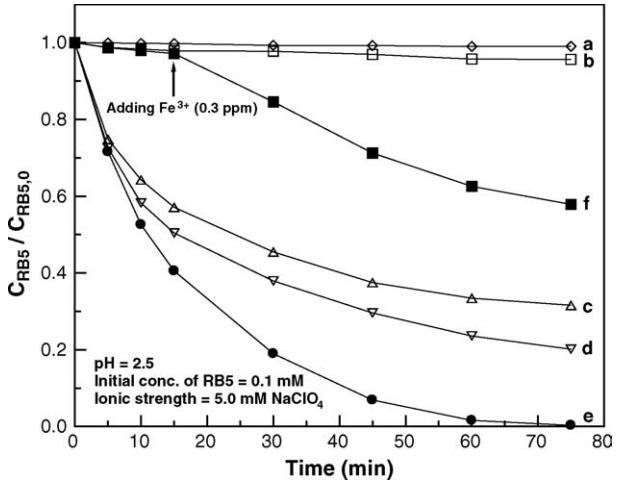

Fig. 6. RB5 concentration as a function of the reaction time under various conditions: (a) without H_2O_2 and iron oxide but with 15 W UVA; (b) without iron oxide but with 5.88 mM H_2O_2 and 15 W UVA; (c) without H_2O_2 but with 2.0 g of FeAA-500 catalyst/L and 15 W UVA; (d) in the dark but with 5.88 mM H_2O_2 and 2.0 g of FeAA-500 catalyst/L; (e) with 5.88 mM H_2O_2, 2.0 g of FeAA-500 catalyst/L, and 15 W UVA; (f) with 0.3 ppm Fe^{3+}, 5.88 mM H_2O_2 and 15 W UVA.

declined, indicating that the degradation of RB5 by photolysis is very limited.

Without a catalyst, but with 5.88 mM H_2O_2 and 15 W UVA (curve b in Fig. 6), the decolorization of RB5 is very limited (<5%) after 90 min of reaction. The decrease in the concentration of RB5 may be caused by oxidation by •OH radicals, which were generated by the direct photolysis of H_2O_2 under UVA.

Without H_2O_2 and 15 W UVA, but with only 2.0 g of FeAA-500/L (curve c), the RB5 concentration decreased to approximately 70% in 90 min, because RB5 was physically adsorbed on the surface of the FeAA-500 catalyst. The point of zero charge (PZC) of Fe_2O_3 is around 6.2 [29], so reducing the pH (<6.2) causes the surface to become positively charged, favoring the adsorption of anionic azo-dye RB5.

Without 15 W UVA but with 5.88 mM H_2O_2 and 2.0 g FeAA-500 catalyst/L in the dark (curve d), after 5 min, the rate of decolorization of RB5 dramatically exceeds that indicated by curve c, because of adsorption and the Fenton-like reaction at the surface of the FeAA-500 catalyst. RB5 is initially adsorbed onto surface of the FeAA-500 catalyst and then oxidized by the •OOH. After some of the intermediates have redissolved from the surface of the catalyst into the solution, the residual RB5 continues to be adsorbed and oxidized. RB5 is degraded fastest in the presence of 2.0 g FeAA-500 catalyst/L, 5.88 mM H_2O_2 and 15 W UVA (curve e in Fig. 6). However, the degradation of RB5 is accelerated by the FeAA-500 catalyst itself or the presence of Fe ions in the solution, because of Fe leaching from the catalyst in an acidic environment, remained to be determined. Accordingly, the change in the concentration of Fe ions in the solution with reaction time was determined using an atomic absorbance spectrophotometer. Fig. 7 presents the results. The graph shows that no Fe ion was present in the solution during the first 15 min, and the Fe concentration increased between 15 and 75 min. At the end of the reaction, the Fe concentration was almost stable at under 0.3 mg/L when 2.0 g of FeAA-500/L was used at pH 2.5, revealing that the FeAA-500 catalyst can be used in industry. Furthermore, an additional experiment, involving the degradation of RB5 in the presence of 0.3 ppm Fe^{3+}, 5.88 mM H_2O_2 and 15 W UVA, was performed to quantify the contribution of the catalyst to the degradation of the RB5, curve f in Fig. 6 shows the results. A careful comparison between the curves clearly indicates that the degradation of RB5 is catalyzed in comes from two perspectives. One is the catalysis from the FeAA-500 catalyst. The other is the catalysis from the Fe ions that leach from the catalyst. However, it should be pointed out that the main contribution is from the FeAA-500 catalyst instead of Fe ions in solution because the initial degradation rate of RB5 (curve e in Fig. 6) is much higher when the FeAA-500 catalyst is used. Accordingly, FeAA-500 exhibits high photo-catalytic activity in the degradation of RB5 but we also believe that Fe ion in solution can accelerate the degradation of RB5.

Fig. 8 plots the changes in the UV–vis spectra during the degradation of RB5 in the presence of the FeAA-500 catalyst and H_2O_2 under UVA light irradiation at pH 2.5 (spectra 1–6). RB5 exhibits characteristic absorption bands at 597 and 391 nm. The absorption peak diminished and disappeared under UVA irradiation, revealing the decolorization of RB5. No new absorption band appeared both in either the visible or the ultraviolet region, indicating the destruction of conjugated structure.

Complete decolorization does not imply that the dye was completely oxidized into CO_2, H_2O and inorganic ions. Reaction intermediates are usually formed and enter solution during degradation. Although identifying the intermediates is very important in determining the reaction path of the degradation of RB5, this study focuses on the extent of mineralization of RB5 with a view to industrial application. Although alternative methods of evaluating the extent of the mineralization of organic pollutants may be available, the removal of TOC is commonly employed in the wastewater treatment industry to specify the extent of mineralization. The TOC removal ratio is defined as,

$$\text{TOC removal ratio} = \left(1 - \frac{\text{TOC}_t}{\text{TOC}_0}\right) \times 100\%,$$

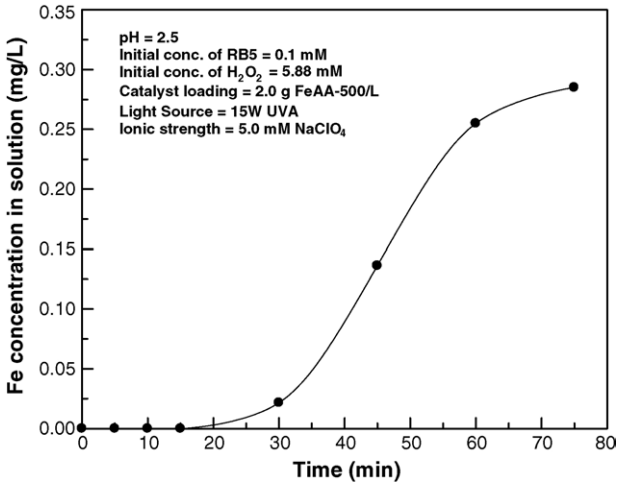

Fig. 7. Fe concentration in solution vs. reaction time.

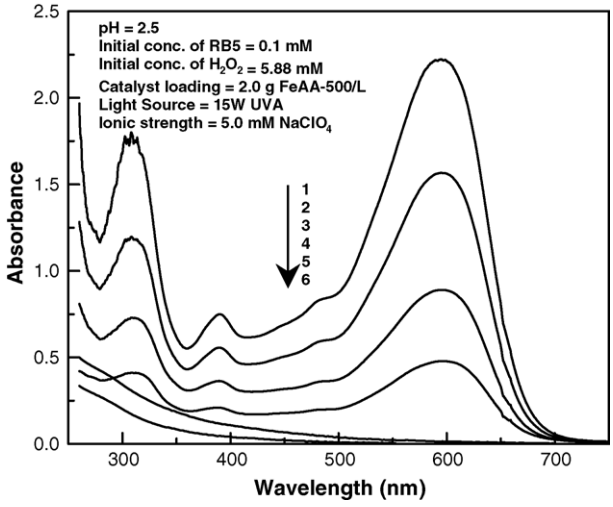

Fig. 8. UV–vis absorption spectral changes of the RB5 (0.1 mM) solution in H_2O_2 (5.88 mM)/FeAA-500 (2.0 g L^{-1}) dispersion under 15 W UVA irradiation; spectra 1–6 denote the reaction time 0, 5, 15, 30, 60 and 75 min at pH 2.5.

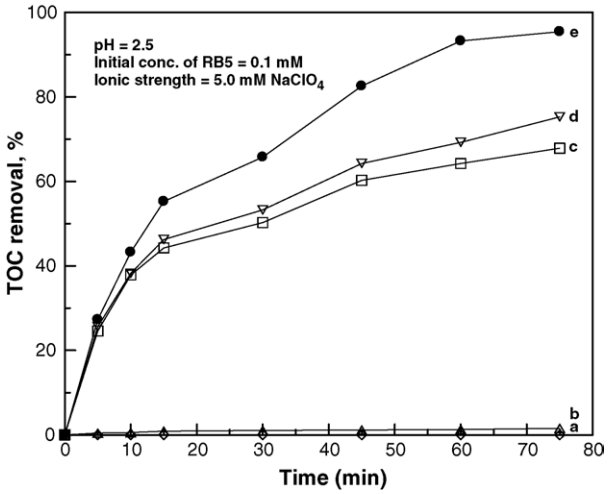

Fig. 9. TOC vs. time under different conditions: (a) without H_2O_2 and iron oxide but with 15 W UVA; (b) without iron oxide but with 5.88 mM H_2O_2 and 15 W UVA; (c) without H_2O_2 but with 2.0 g of FeAA-500 catalyst/L and 15 W UVA; (d) in the dark but with 5.88 mM H_2O_2 and 2.0 g of FeAA-500 catalyst/L; (e) with 5.88 mM H_2O_2, 2.0 g of FeAA-500 catalyst/L, and 15 W UVA.

where TOC_t and TOC_0 are the values of TOC at reaction times t and 0, respectively.

Fig. 9 plots the measured TOC removal ratio against irradiation time under various conditions. The figure reveals three important conclusions. First, without the FeAA-500 catalyst but with 5.88 mM H_2O_2 and 15 W UVA (curve b in Fig. 9), only around 1.5% of TOC is removed after 75 min of reaction, revealing that the amount of $^{\bullet}OH$ generated directly by the photolysis of H_2O_2 by UVA light is very small. Second, the difference between the extent of TOC removal indicated by curve c and that indicated by curve d was only approximately 7% after 75 min, revealing that the $^{\bullet}OOH$ generated by the Fenton-like reaction of Fe^{3+} on the surface of the FeAA-500 catalyst cannot effectively mineralize RB5 into H_2O and CO_2. The authors made similar observations in another study [30]. Third, when the 15 W UVA light was turned on (curve e in Fig. 9), significantly increased the rate of TOC removal, especially after 5 min of reaction. Compare curves e (light) and d (dark) reveal that approximately 95% and 75% TOC, respectively, are removed after 75 min reaction time, indicating that the presence of UVA light effectively promotes the mineralization of RB5.

4. Conclusions

A novel FeAA-500 catalyst was prepared by fluidized-bed reactor (FBR) crystallization. XRD analysis indicated that the FeAA-500 catalyst consists mainly of Fe_2O_3 (hematite) crystallite. FeAA-500 was developed as a catalyst of the photooxidative degradation of 0.1 mM RB5 in the presence of H_2O_2 and UVA light in a solution with a pH of 2.5. The model pollutant RB5 was completely decolorized and the total organic carbon (TOC) removal ratio was 95% after 75 min of reaction. Results of this study demonstrate that the FeAA-500 catalyst exhibits not only high photo-catalytic activity but also high stability in an acidic environment. Therefore, FeAA-500 has potential as a heterogeneous catalyst of the photooxidative degradation of organic compounds.

Acknowledgement

The authors would like to thank the National Science Council of Taiwan, Republic of China, for financially supporting this research under Contract No. NSC93-2622-E-006-026-CC3.

References

[1] M.S. Bahorsky, Water Environ. Res. 69 (1997) 658.
[2] D.K. Cha, J.S. Song, D. Sarr, B.J. Kim, Water Environ. Res. 68 (1996) 575.
[3] S.F. Kang, C.H. Liao, M.C. Chen, Chemosphere 46 (2002) 923.
[4] J.A. Theruvathu, C.T. Aravindakumar, R. Flyunt, J.V. Sonntag, C.V. Sonntag, J. Am. Chem. Soc. 123 (2001) 9007.
[5] B.D. Lee, M. Hosomi, Water Res. 35 (2001) 2314.
[6] J.J. Pignatello, Environ. Sci. Technol. 26 (1992) 944.
[7] G. Ruppert, R. Bauer, G. Heisler, S. Novalic, Chemosphere 27 (1993) 1339.
[8] J. Kiwi, C. Pulgarin, P. Peringer, Appl. Catal. B: Environ. 3 (1994) 335.
[9] M.E. Balmer, B. Sulzberger, Environ. Sci. Technol. 33 (1999) 2418.
[10] K. Wu, Y. Xie, J. Zhao, H. Hidaka, J. Mol. Catal. A: Chem. 144 (1999) 77.
[11] P.L. Huston, J.J. Pignatello, Environ. Sci. Technol. 30 (1996) 3457.
[12] W. Gernjk, T. Krutzler, A. Glaser, S. Malato, J. Caceres, R. Bauer, A.R. Fernandez-Alba, Chemosphere 50 (2003) 71.
[13] S. Parra, I. Guasaquillo, O. Enea, E. Mielczarski, J. Mielczarki, P. Albers, L. Kiwi-Minsker, J. Kiwi, J. Phys. Chem. B 107 (2003) 7026.
[14] J. Fernandez, J. Bandara, A. Lopez, P. Alberz, J. Kiwi, Chem. Commun. (1998) 1493.
[15] J. Fernandez, J. Bandara, A. Lopez, Ph. Buffar, J. Kiwi, Langmuir 15 (1999) 185.
[16] J. Fernandez, M.R. Djananjeyan, J. Kiwi, Y. Senuma, J. Hilborn, J. Phys. Chem. 104 (2000) 5298.
[17] M.R. Djananjeyan, J. Kiwi, P. Albers, O. Enea, Helv. Chim. Acta 84 (2001) 3433.
[18] A. Bozzi, T. Yuranova, J. Mielczarski, A. Lopez, J. Kiwi, Chem. Commun. (2002) 2202.
[19] J. Feng, X. Hu, P.L. Yue, H.Y. Zhu, G.Q. Lu, Ind. Eng. Chem. Res. 42 (2003) 2058.
[20] J. Feng, X. Hu, P.L. Yue, H.Y. Zhu, G.Q. Lu, Chem. Eng. Sci. 58 (2003) 679.
[21] J. Feng, X. Hu, P.L. Yue, H.Y. Zhu, G.Q. Lu, Water Res. 37 (2003) 3776.
[22] J. Feng, X. Hu, P.L. Yue, Environ. Sci. Technol. 38 (2004) 269.
[23] Y.H. Huang, G.H. Huang, S. Chou, H.S. Perng, A pending ROC Patent 87,106,787 (1998).
[24] Y.H. Huang, G.H. Huang, S.S. Chou, H.S. You, S.H. Perng, US Patent: 6,143,182 (2000).
[25] S. Chou, C. Huang, Y.H. Huang, Chemosphere 39 (1999) 1997.
[26] S. Chou, C. Huang, Y.H. Huang, Environ. Sci. Technol. 35 (2001) 1247.
[27] S. Chou, C. Huang, Chemosphere 38 (1999) 2719.
[28] I. Arslan, I. Akmehmet Balciogglu, Dyes Pigments 43 (1999) 95.
[29] S. Mustafa, S. Tasleem, A. Naeem, J. Colloid Interface Sci. 275 (2004) 523.
[30] C.L. Hsueh, Y.H. Huang, C.C. Wang, C.Y. Chen, Chemosphere 58 (2005) 1409.